ADAPTIVE MATCHED SUBSPACE DETECTORS FOR HYPERSPECTRAL IMAGING APPLICATIONS

Dimitris Manolakis, Christina Siracusa, and Gary Shaw

MIT Lincoln Laboratory
244 Wood Street, Lexington, MA 02420-9185.
E-mail: dmanolakis@ll.mit.edu

ABSTRACT

Real-time detection and identification of man-made objects or materials ("targets") from airborne platforms using hyperspectral sensors are of great interest for civilian and military applications. Over the past several years, different algorithms for the detection of targets with known spectral signature have been developed. Most of these algorithms have been reviewed in [1] within a unified theoretical and notational framework. In this paper we study adaptive matched subspace detection algorithms for low probability, single-pixel or subpixel targets. These algorithms explore the linear mixing model to both specify the desired target and characterize the interfering background. The derived algorithms are theoretically and experimentally evaluated with regard to two desirable properties: capacity to operate in constant false alarm rate (CFAR) mode and target "visibility" enhancement. Furthermore, an approach is presented for taking into account target variability, when present, to improve detection.

1. INTRODUCTION

A key element of hyperspectral imaging (HSI) data exploitation is imaging spectroscopy, i.e., the identification of materials based on how they absorb and reflect light. In this sense, HSI data processing attempts to accomplish from a distance what a chemical spectroscopist does in the laboratory. Within the instantaneous field of view of the sensor mixtures of materials are expected, due to the physical size of the image pixel and the composition of natural scenes. Therefore, the spectrum of an individual pixel is a mixture of the individual spectra of the materials present in the pixel.

The subject of this paper is the design and analysis of algorithms for the detection of pixel or subpixel targets with known spectral signature in the presence of interfering background and noise. In Section 2 we formulate the subpixel target detection problem using the linear mixing model and the concepts of target and background subspaces. We also discuss procedures for the specification of the target subspace and the estimation of the background subspace. In Section 3 we use a geometrical approach to develop the adaptive matched subspace detector and characterize its performance for Gaussian noise using the postulated linear mixing model and the generalized likelihood ratio. The widely used orthogonal subspace projection algorithm [2] and the matched filter algorithm for known signals in white noise [3] are then derived by using obvious simplifications and approximations. Finally, in Section 4, we experimentally evaluate the performance of the various algorithms using hyperspectral data collected with the HYDICE sensor.

This work was sponsored by the Department of the Defense Air Force contract F19628-95-C-0002. Opinions, interpretations, conclusions, and recommendations are those of the author and not necessarily endorsed by the United States Air Force.

2. THE LINEAR MIXING MODEL

In the linear mixing model (LMM), the spectrum of a mixed pixel is represented [4] as a linear combination of component spectra (end members). The weight of each end member spectrum (abundance) is proportional to the fraction of the pixel area covered by the end member. By definition, abundances should be nonnegative and should sum to one. If there are L spectral bands, the spectrum of the pixel and the spectra of the end members can be represented by L-dimensional vectors. In subpixel target detection, we wish to determine if a pixel, $\boldsymbol{x}$, contains some material (target) characterized by either a single spectral signature or a linear combination of spectral signatures. When the target is present, the spectrum of an observed pixel can be decomposed into two components as

$$\boldsymbol{x} = \sum_{k=1}^{M} a_k \boldsymbol{s}_k + \boldsymbol{w} = \underbrace{\sum_{k=1}^{P} a_k \boldsymbol{s}_k}_{\text{Target } \boldsymbol{s}_\mathrm{t}} + \underbrace{\sum_{k=P+1}^{M} a_k \boldsymbol{s}_k}_{\text{Background } \boldsymbol{s}_\mathrm{b}} + \boldsymbol{w} \qquad (1)$$

using the LMM. If $\boldsymbol{S}_\mathrm{t}$ and $\boldsymbol{S}_\mathrm{b}$ are the matrices formed by the first P and the last Q columns of $\boldsymbol{S}$ ($M = P + Q$), we can write (1) in matrix form as

$$\boldsymbol{x} = \boldsymbol{S}\boldsymbol{a} + \boldsymbol{w} \triangleq \boldsymbol{S}_\mathrm{t}\boldsymbol{a}_\mathrm{t} + \boldsymbol{S}_\mathrm{b}\boldsymbol{a}_\mathrm{b} + \boldsymbol{w} \qquad (2)$$

where $\boldsymbol{a}_\mathrm{t}$ and $\boldsymbol{a}_\mathrm{b}$ consist of the first P and the last Q components of $\boldsymbol{a}$, respectively. Since $\boldsymbol{s}_\mathrm{t} = \boldsymbol{S}_\mathrm{t}\boldsymbol{a}_\mathrm{t}$ we say that the target lies in a P-dimensional subspace $\langle \boldsymbol{S}_\mathrm{t} \rangle$ of $\mathbb{R}^L$ specified by the columns of $\boldsymbol{S}_\mathrm{t}$ (target subspace). Similarly, the Q-dimensional subspace $\langle \boldsymbol{S}_\mathrm{b} \rangle$ of $\mathbb{R}^L$, specified by the columns of $\boldsymbol{S}_\mathrm{b}$, is known as the background subspace.

The target subspace should be specified by the user, whereas the background subspace should be estimated from the data currently available to the detector. Due to changes in atmospheric conditions, sensor geometry, and surface defects, a target spectral signature can exhibit significant variability. If we have available a multitude of target spectrum observations, say $\boldsymbol{x}_\mathrm{t}(n)$, $n = 1, 2, \ldots, N_\mathrm{t}$, we can model target variability and use it in the detection algorithm to improve robustness. In this paper, we account for this variability by finding an orthogonal basis that spans, with sufficient accuracy, the subspace spanned by the target vectors. These basis vectors constitute the columns of the target subspace matrix $\boldsymbol{S}_\mathrm{t}$. The background subspace matrix $\boldsymbol{S}_\mathrm{b}$ can be estimated from the HSI cube using the eigenvectors [5] of the HSI cube correlation matrix $\hat{\boldsymbol{R}}_x = \boldsymbol{X}^T\boldsymbol{X}/N$ or, equivalently, the singular vectors of the data matrix $\boldsymbol{X}^T$. We form the matrix, $\boldsymbol{S}_\mathrm{b}$, using the first Q significant eigenvectors of $\boldsymbol{R}_x$. It should be stressed at this point that there is no one-to-one correspondence between the estimated $\boldsymbol{S}_\mathrm{b}$ and spectral properties. The lack of one-to-one correspondence is not a problem for detection applications as long as $\boldsymbol{S}_\mathrm{b}$ provides a good statistical approximation of the background and there is no leakage from the target subspace to the background subspace.

3. THE ADAPTIVE MATCHED SUBSPACE DETECTOR (AMSD)

When the target and background subspaces are available, the target detection problem involves choosing between the hypotheses

$$\begin{aligned} H_0: &\quad \boldsymbol{x} = \boldsymbol{S}_\mathrm{b}\boldsymbol{a}_\mathrm{b} + \boldsymbol{w}, \quad \boldsymbol{w} \sim \mathcal{N}(\boldsymbol{0}, \sigma_w^2\boldsymbol{I}) \quad \text{(Target absent)} \\ H_1: &\quad \boldsymbol{x} = \boldsymbol{S}_\mathrm{t}\boldsymbol{a}_\mathrm{t} + \boldsymbol{S}_\mathrm{b}\boldsymbol{a}_\mathrm{b} + \boldsymbol{w} = \boldsymbol{S}\boldsymbol{a} + \boldsymbol{w} \quad \text{(Target present)} \end{aligned} \tag{3}$$

which is equivalent to choosing between the "full" LMM $\boldsymbol{x} = \boldsymbol{S}\boldsymbol{a} + \boldsymbol{w}$ and the "reduced" LMM $\boldsymbol{x} = \boldsymbol{S}_\mathrm{b}\boldsymbol{a}_\mathrm{b} + \boldsymbol{w}$.

Under the white Gaussian noise assumption, the maximum likelihood estimates (MLEs) of $\boldsymbol{a}_\mathrm{t}$, $\boldsymbol{a}_\mathrm{b}$, and σ_w^2 are identical to the least-squares (LS) estimates. The fit of each model is measured by the sum of squared errors (SSE), which is equal to the length of the perpendicular from the tip of $\boldsymbol{x}$ to the background subspace or the combined target and background subspace, respectively (see Figure 1). In fact, the

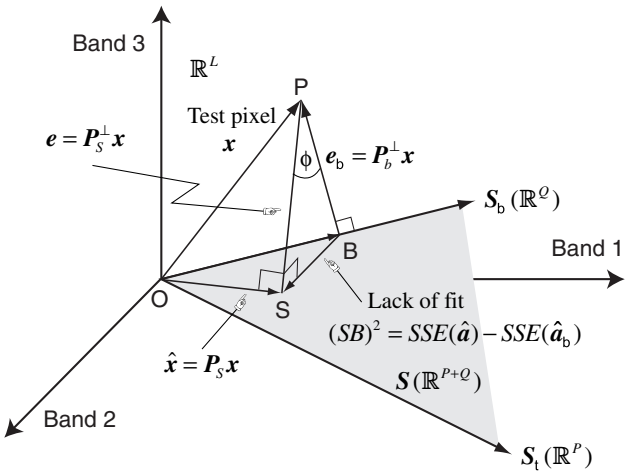

Fig. 1. Geometrical illustration of subspace matched filter detection.

generalized likelihood ratio test is given by

$$\mathcal{L}(\boldsymbol{x}) = \left[\frac{\mathrm{SSE}(\hat{\boldsymbol{a}}_\mathrm{b})}{\mathrm{SSE}(\hat{\boldsymbol{a}})}\right]^{L/2} = \left(\frac{\boldsymbol{x}^T\boldsymbol{P}_\mathrm{b}^\perp\boldsymbol{x}}{\boldsymbol{x}^T\boldsymbol{P}_S^\perp\boldsymbol{x}}\right)^{L/2} = (\cos\phi)^{-L} \tag{4}$$

which can be used to obtain a target detection algorithm. The matrix $\boldsymbol{P}_S \triangleq \boldsymbol{S}(\boldsymbol{S}^T\boldsymbol{S})^{-1}\boldsymbol{S}^T$ is known as the *projection* matrix and $\boldsymbol{P}_S^\perp \triangleq \boldsymbol{I} - \boldsymbol{P}_S$ as the orthogonal projection error matrix. The error or residual vector is obtained by $\boldsymbol{e} = \boldsymbol{x} - \hat{\boldsymbol{x}} = \boldsymbol{P}_S^\perp\boldsymbol{x}$. Similar formulas hold for the background subspace matrix $\boldsymbol{S}_\mathrm{b}$. Since $\mathrm{SSE}(\hat{\boldsymbol{a}}) \leq \mathrm{SSE}(\hat{\boldsymbol{a}}_\mathrm{b})$, we have $\mathcal{L}(\boldsymbol{x}) \geq 1$. To make a decision we need to compare $\mathcal{L}(\boldsymbol{x})$ to a given threshold ℓ_0 and decide H_1 when $\mathcal{L}(\boldsymbol{x}) \geq \ell_0$ and H_0 otherwise. Since the threshold determines both P_D and P_{FA}, we need to determine the probability distribution of $\mathrm{GLR}(\boldsymbol{x})$. Since PS$\perp$SB, the random vectors $\boldsymbol{e} = \boldsymbol{P}_S^\perp\boldsymbol{x}$ and $\overrightarrow{\mathrm{BS}} = \boldsymbol{e}_\mathrm{b} - \boldsymbol{e} = (\boldsymbol{P}_\mathrm{b}^\perp - \boldsymbol{P}_S^\perp)\boldsymbol{x}$ are orthogonal (that is uncorrelated). Furthermore, since $\boldsymbol{e}$ and $\overrightarrow{\mathrm{BS}}$ are normal (as linear transformations of normal vector $\boldsymbol{x}$) they are also independent. Therefore, in practice we use the ratio

$$\begin{aligned} T_\mathrm{AMSD}(\boldsymbol{x}) &\triangleq \frac{\boldsymbol{x}^T(\boldsymbol{P}_\mathrm{b}^\perp - \boldsymbol{P}_S^\perp)\boldsymbol{x}}{\boldsymbol{x}^T\boldsymbol{P}_S^\perp\boldsymbol{x}} = \frac{(\mathrm{BS})^2}{(\mathrm{PS})^2} \\ &= (\tan\phi)^2 = [\mathcal{L}(\boldsymbol{x})]^{2/L} - 1 \end{aligned} \tag{5}$$

whose distribution can be more easily determined due to the independence of numerator and denominator terms. Indeed, it can be shown [3, 6] that $\boldsymbol{x}^T(\boldsymbol{P}_\mathrm{b}^\perp - \boldsymbol{P}_S^\perp)\boldsymbol{x}/(\sigma_w^2 P) \sim x_P^2(\mathrm{SINR_o})$ and $\boldsymbol{x}^T\boldsymbol{P}_S^\perp\boldsymbol{x}/\left[\sigma_w^2(L-P-Q)\right] \sim x_{L-P-Q}^2(0)$. Note that $(\mathrm{BS})^2 = \|\boldsymbol{e}_\mathrm{b}\|^2 - \|\boldsymbol{e}\|^2$ and $(\mathrm{PS})^2 = \|\boldsymbol{e}\|^2$. Since

the two quadratic forms are independent

$$T(\boldsymbol{x}) = \frac{(\mathrm{BS})^2}{(\mathrm{PS})^2} \frac{L-P-Q}{P} \sim F_{P,L-P-Q}(\mathrm{SINR_o}) \quad (6)$$

where $F_{P,L-P-Q}(\mathrm{SINR_o})$ is noncentral F distribution with P numerator degrees of freedom, $L-P-Q$ denominator degrees of freedom, and noncentrality parameter $\mathrm{SINR_o}$

$$\mathrm{SINR_o} = \frac{(\boldsymbol{S}_\mathrm{t}\boldsymbol{a}_\mathrm{t})^T \boldsymbol{P}_\mathrm{b}^\perp (\boldsymbol{S}_\mathrm{t}\boldsymbol{a}_\mathrm{t})}{\sigma_w^2} = \frac{\left\| \boldsymbol{P}_\mathrm{b}^\perp (\boldsymbol{S}_\mathrm{t}\boldsymbol{a}_\mathrm{t}) \right\|^2}{\sigma_w^2} \quad (7)$$

Since the term $\boldsymbol{P}_\mathrm{b}^\perp(\boldsymbol{S}_\mathrm{t}\boldsymbol{a}_\mathrm{t})$ is the component of the target which is orthogonal to the background subspace, $\mathrm{SINR_o}$ can be interpreted as the theoretical signal to interference-plus-noise ratio. In the statistical literature $T(\boldsymbol{x})$ is denoted by $F(\boldsymbol{x})$ and is known as the F-test[1]. The detection test is given by

$$T(\boldsymbol{x}) = \frac{(\mathrm{BS})^2}{(\mathrm{PS})^2} \frac{L-P-Q}{P} \underset{H_0}{\overset{H_1}{\gtrless}} \eta_0 \quad (8)$$

where the threshold η_0 is specified[2] by the required probability of false alarm

$$P_\mathrm{FA} = 1 - F_{P,L-P-Q}(0, \eta_0) \quad (9)$$

because $\mathrm{SINR_o} = 0$ under H_0. Since the distribution of $T(\boldsymbol{x})$ under H_0 is known, we can set the threshold η_0 to attain CFAR operation. The probability of detection

$$P_\mathrm{D} = 1 - F_{P,L-P-Q}(\mathrm{SINR_o}, \eta_0) \quad (10)$$

depends on the unknown $\boldsymbol{a}_\mathrm{t}$, σ_w^2 and therefore it cannot be maximized to obtain an optimum Neyman-Pearson detector.

Plots derived from the above relations [1] show that performance deteriorates as the dimensionality of the target subspace increases (that is as the a-priori information about the target decreases) as expected. For a given probability of detection, there is a loss in SINR due to the need to estimate the target abundance (clairvoyant detector) plus the noise variance (adaptive detector). As is intuitively expected, performance improves as the number of band increases, that is as we supply more information into the detector. It can be shown that, independent of the normality assumption, the detectors maximize the signal to interference ratio [3].

Special cases When $P = 1$ the abundance of the target is given by

$$\hat{a}_\mathrm{t} = \frac{\boldsymbol{s}_\mathrm{t}^T \boldsymbol{P}_\mathrm{b}^\perp \boldsymbol{x}}{\boldsymbol{s}_\mathrm{t}^T \boldsymbol{P}_\mathrm{b}^\perp \boldsymbol{s}_\mathrm{t}} \sim \mathcal{N}(a_\mathrm{t}, \sigma_w^2 \boldsymbol{s}_\mathrm{t}^T \boldsymbol{P}_\mathrm{b}^\perp \boldsymbol{s}_\mathrm{t}) \,. \quad (11)$$

[1]The $\mathcal{L}(\boldsymbol{x})$ and $T(\boldsymbol{x})$ tests are monotonically related, and the distribution of the GLRT can be expressed in terms of the beta distribution by exploiting its relationship with the F distribution [7].

[2]With a slight abuse of notation, we use $F_{P,L-P-Q}(\mathrm{SINR_o}, \eta_0)$ to denote the cumulative distribution function of the non-central F random variable.

The numerator of the abundance estimator (11) has been proposed in [2] as a detection statistic under the name Orthogonal Subspace Projection (OSP) algorithm. However, it is better to use the normalized statistic $T_\mathrm{OSP}(\boldsymbol{x}) = \hat{a}_\mathrm{t}$ because it corresponds to the abundance estimate for the desired target. The resulting algorithm is not CFAR because the abundance of the target and the variance of the sensor noise are unknown. Clearly, the theoretically predicted Gaussian distribution of the target abundance conflicts with the physical constraint $0 \le a_\mathrm{t} \le 1$.

If there is no background, or we choose to ignore its existence, i.e., we set $\boldsymbol{S}_\mathrm{b} = \boldsymbol{0}$, the statistic (5) reduces to

$$T_\mathrm{MF}(\boldsymbol{x}) = T_\mathrm{AMSD}(\boldsymbol{x})|_{\boldsymbol{S}_\mathrm{b}=\boldsymbol{0}} = \frac{\boldsymbol{x}^T \boldsymbol{P}_\mathrm{t} \boldsymbol{x}}{\boldsymbol{x}^T \boldsymbol{P}_\mathrm{t}^\perp \boldsymbol{x}} \quad (12)$$

which is the well-known matched filter[3] for signals in white noise.

4. EXPERIMENTAL RESULTS

To assess the performance of the different algorithms, we use the Forest Radiance I data collected with the HYDICE sensor. Although, we have experimented with different background and target data, for illustration purposes we shall use a relatively homogeneous grass scene consisting of (97x80) pixels. The number of bands used is $L = 144$. With regard to targets, we have chosen a target with 45 pixels consisting of a single material. We determine the target template $\boldsymbol{s}_\mathrm{t}$ required for the implementation of each detection algorithm in two different ways: (a) using the mean value of the target pixels and (b) using the first P left-singular vectors of the target pixel matrix to define a target subspace (this approach takes into account the variability of the target).

The estimate of the background subspace $\hat{\boldsymbol{S}}_\mathrm{b}$ was obtained using the first $Q = 5$ significant eigenvectors of the estimated correlation matrix of the background pixels (the "known" target pixels were excluded). These eigenvectors capture more than 99 percent of the data cube energy in each case.

To investigate the performance of the three detectors, we assess their capacity (a) to accurately model the background statistics , (b) to enhance the "visibility" of the desired target (background-target separation), and (c) to take into account and effectively explore target variability. Figure 2 compares the experimental detection statistics to the theoretically predicted one for the AMSD detector operating against a grass background. We show the AMSD algorithm only, because it is CFAR for normal data. Figure 3 shows the detection

[3]The typical matched filter for known signals in color interference-plus-noise, which is specified in terms of the covariance matrix, is known in the hyperspectral literature as the constrained energy maximization (CEM) algorithm [2]

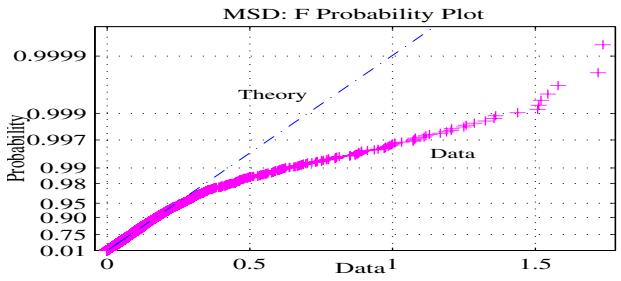

Fig. 2. Background (grass) detection statistics modeling for the AMSD detector.

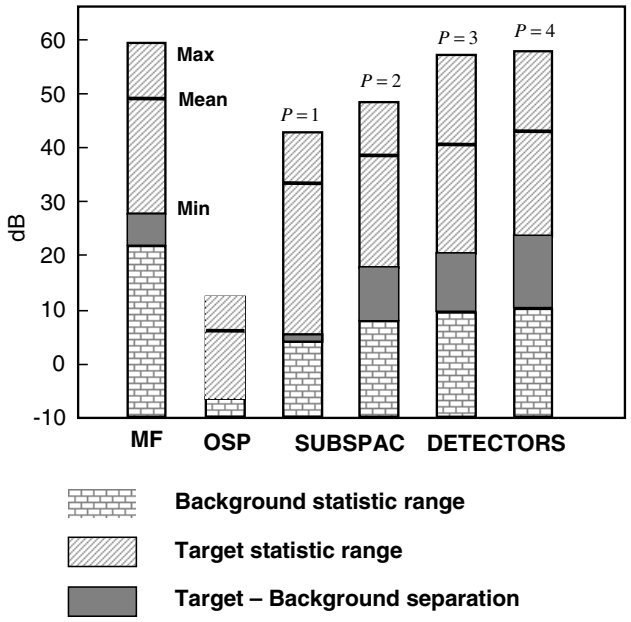

Fig. 3. Target-background separability for the different detection algorithms. The AMSD is shown for different values of target subspace dimensionality.

statistic of the target and the maximum value of the background detection statistics for the various detectors in a grass background. The mean of the target pixels is almost identical to the first singular vector. Therefore, the first three bars show performance when either the mean or the first singular vector are used as known target signature. These and many other similar results indicate the superior performance of the AMSD. However, the background detection statistics do not always agree with the theoretical predictions, underlining the need for more appropriate (non-Gaussian) statistical models.

5. CONCLUSIONS

In this paper we presented a class of adaptive subspace detection algorithms for subpixel hyperspectral targets with known spectral signature. We provided theoretical and experimental results clarifying the performance of these detectors and illustrated how to exploit target variability, when present, to improve the detection performance of the more sophisticated AMSD algorithm.

Acknowledgments We wish to express our gratitude to Captain Frank Garcia, DUSD (S&T), program manager HTAP, for his enthusiastic support. We also express our gratitude to Spectral Information Technology Applications Center (SITAC) for providing the HYDICE data used in this work.

6. REFERENCES

[1] D. Manolakis, G. Shaw, and N. Keshava, "Comparative analysis of hyperspectral adaptive matched filter detectors," in *Algorithms for Multispectral and Hyperspectral Imagery*, Orlando, FL, April 2000, SPIE.

[2] J. C. Harsanyi and C. I. Chang, "Detection of low probability subpixel targets in hyperspectral image sequences with unknown backgrounds," *IEEE Trans. Geoscience and Remote Sensing*, vol. 32, no. 4, pp. 779–785, July 1994.

[3] S. M. Kay, *Fundamentals of Statistical Signal Processing*, Prentice Hall, New Jersey, 1998.

[4] J. B. Adams, M. O. Smith, and A. R. Gillespie, "Remote geochemical analysis: Elemental and mineralogical composition," in *Imaging spectroscopy: Interpretation based on spectral mixture analysis*, C. M. Pieters and P. A. J. Englert, Eds., Cambridge, 1993, pp. 145–166, Cambridge University Press.

[5] W. H. Farrand and J. C. Harsanyi, "Discrimination of poorly exposed lithologies in imaging spectrometer data," *Journal of Geophysical Research*, vol. 100, no. E1, pp. 1565–1578, January 1995.

[6] L. L. Scharf and B. Friedlander, "Matched subspace detectors," *IEEE Trans. on Signal Processing*, vol. 42, no. 8, pp. 2146–2157, August 1994.

[7] R. R. Hocking, *Methods and Applications of Linear Models*, Wiley, New York, 1996.